A new Investigation Methodology to predict Far Field Radiated Immunity from Near Field Scan Immunity Measurements

André Durier, Sonia Ben Dhia, Alexandre Boyer, Tristan Dubois

A new Investigation Methodology to predict Far Field Radiated Immunity from Near Field Scan Immunity Measurements

André DURIER
Qualification Laboratories EMC
Continental Automotive France
Toulouse, France
andre.2.durier@continental-corporation.com

Sonia BEN DHIA, Alexandre BOYER
LAAS-CNRS, INSA Toulouse
Toulouse, France
sonia.bendhia@insa-toulouse.fr
Alexandre.boyer@ina-toulouse.fr

Tristan DUBOIS
IMS Bordeaux
Bordeaux, France
tristan.dubois@ims-bordeaux.fr

***Abstract*— The increasing complexity of embedded calculators in terrestrial vehicles makes more and more complex their qualification for Electromagnetic Compatibility. The cost of test facilities and certified personnel for a normative test in Radiated Immunity (RI) is high and constitutes a bottleneck for Original Equipment Manufacturers (OEM). To solve their problem, OEM need a quick, economical and easy-to-use investigative system. The Near Field Scan Immunity (NFSI) method is quite fitted to be a good investigation tool when used with immunity probe dedicated to investigation at Printed Circuit Board (PCB) level. But, to be able to compare NFSI measurements to RI ones, problems inherent in NFSI measurement as its dependency to probe's position and the non-consideration of the harness resonances seen during the RI measurement must be solved. This paper presents a methodology to predict the RI immunity level of an equipment after layout or component change from a RI measurement performed on original equipment and NFSI measurement performed on both versions.**

Keywords— Near Field Scan Immunity probe, Radiated Immunity prediction from Near Field Scan Immunity measurements,

I. INTRODUCTION

According to national or international regulations concerning the Electromagnetic Compatibility, all terrestrial motor vehicles must be approved and certified by an independent laboratory according standardized tests methods To prevent any non-compliance during vehicle certification, car manufacturers proceed themselves to the qualification of their vehicles and require from their suppliers specific qualification tests at equipment level standardized by the ISO (International Standard Organization). Finally, to achieve the requirements given by the car manufacturer, equipment suppliers require to their integrated circuit (IC) manufacturers specific tests performed at IC level according test methods standardized by the IEC (International Electrotechnical Commission). The Fig. 1 illustrates the tests methods used at vehicle, equipment and IC level for the radiated immunity.

At equipment level, the ISO 11452-2 [1] Absorber lined shielded enclosure (ALSE) test method is commonly used by electronic suppliers to measure the Radiated Immunity level. The method consists to illuminate the equipment under test (EUT) linked to its representative loads thru an electrical harness with an electromagnetic (EM) plane wave characterized by its E-field strength and its polarization. The failures occurring during the RI test are mainly due to currents induced into the harness exposed to the EM field flowing into the equipment and reaching IC.

Fig. 1. Radiated immunity test methods at vehicle, equipment & IC level

At IC level, the NFSI [2] test method is one of the methods used by component manufacturers to measure the Radiated Immunity level. In numerous papers e.g [3] NFSI method has been compared to the Direct Power Injection (DPI) [4] method and to TEM cell and Wideband TEM Cell method [5]. Despite developed for IC radiated immunity measurement, this method is also applicable at PCB level as stated e.g in [6]. The NFSI test setup is very similar to that used in RI. The antenna is replaced by an immunity probe placed on a robotics system allowing its movement on 3 axes. The immunity probe locally produces high electric and/or magnetic fields and failures occurring during the NFSI test are mainly due to the currents induced into the PCB traces and reaching IC.

A reliable extrapolation of a measurement performed in near field to evaluate the level of susceptibility in far field is presented in [7]. E & H-fields generated by the NFSI probe above the DUT are calculated and compared to the fields generated during the RI test. But the practical use of this method is limited due to the high number of measurements to be done and the need to measure the phase also. Moreover, this method does not consider the coupling of the far field on the harness linking the DUT to its loads.

The methodology described in this paper has been developed to meet a specific industrial need: to predict the

radiated immunity level of an equipment after a PCB design change without proceeding to a full requalification of the modified equipment. To achieve this goal, the methodology proposes to use the result of the RI measurement performed on the initial equipment and the result of NFSI measurements performed on initial and modified equipment.

This paper is the result of an experimental approach based on the comparison of voltage induced on loads placed on a PCB during RI and NFSI measurements for different configurations. We present in the Section II a comparison of the immunity levels obtained during NFSI and RI tests on a PCB composed of coupled microstrip lines. The methodology is described in Section III in case of design changes. Conclusions on advantages and drawbacks of the methodology and some perspectives for further improvement are given in Section IV.

II. Comparison of Far Field and Near Field Measurements on a Simple Test Case

A. Test Case Description

The PCB used for demonstration is willingly very simple to be able to easily explain the methodology developed in Section III. It allows to place loads at PCB microstrip line ends and filtering components at PCB input.

Fig.2 illustrates the test case constituted by a ~70±3 cm long 5-wire harness linking a demonstrator PCB to its loads. The harness is made up of 5 single conductor wires for the signals and the ground. The demonstrator PCB is composed by 4 microstrip lines (T1-T4) routed in parallel upon a ground plane. The lines width is 150 µm and the gap between lines T1 and T2, lines T2 and T3 and lines T3 and T4 is respectively 300 µm, 150 µm and 900 µm. Microstrip line characteristic impedance is 97 Ω. The load box is composed of 100 Ω placed between each signal wire termination and the ground wire.

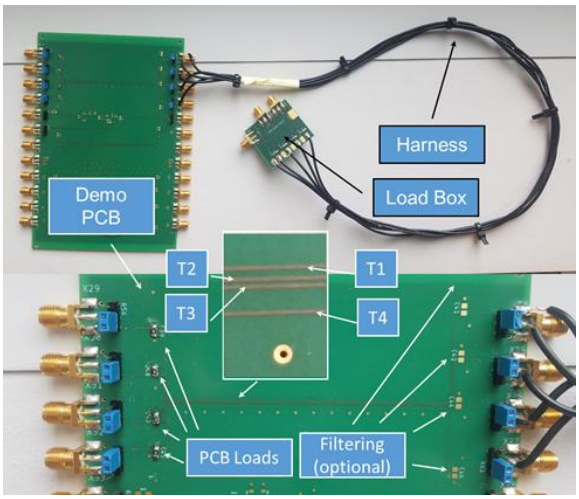

Fig. 2. PCB demonstrator

Some SMD loads are placed on the PCB at the end of each microstrip line and optional filtering components could be placed at their input. We studied three configurations:

- Conf#1 : PCB load = 1 kΩ, no filtering
- Conf#2 : PCB load = 10 kΩ, filtering = 10 nF
- Conf#3 : PCB load = 10 kΩ in parallel with 10 nF

The measurements of the induced voltage have been performed on the PCB loads placed on the most coupled line T2 and on the less coupled line T4 with a 50 Ω power meter described in [8]. The power meter is placed on the SMA connector situated at PCB trace termination.

B. Radiated Immunity Test Results

During RI test, the harness, PCB and load box lie on a ~50 mm thick insulator (εr = 1.2) placed on a metallic table. A 3D E-field sensor is placed above the harness allowing the normalization of the measured induced voltage on a 1 V/m measured E-Field. The measurement is achieved with a frequency step of 20 MHz for F < 1 GHz and 50 MHz for F > 1 GHz for vertical and horizontal polarization of the E-Field.

Fig.3 illustrates the normalized induced voltages on the load placed at the end of the line T2 (Max T2) and on the load placed at the end of the line T4 (Max T4) measured during a RI test for the Conf #2. The maximum value of the measured induced voltages for both polarizations is taken into account.

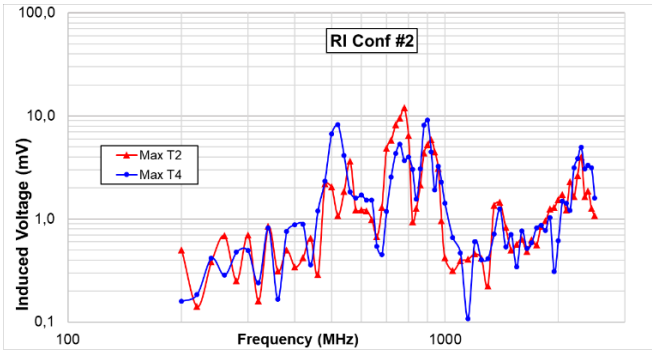

Fig. 3. Normalized induced voltages measured during RI (Conf #2)

We clearly observe in Fig.3 the effect of the 10 nF filtering capacitor placed at the T2 and T4 traces input. The voltage induced on the load placed at the trace terminations is low while the impedance of the 10 nF capacitor is low and increases when the impedance of the capacitor increases due to the parasitic inductance. Voltage maxima observed in Fig.3 seem to correspond to harness resonances occurring when the wavelength of the perturbation equals an odd multiple of the quarter of the harness length.

C. Near Field Scan Immunity Test Results

The same harness, PCB and load box, as for RI measurement, lie on a ~50 mm thick dielectric. A coplanar magnetic field immunity probe, specifically developed for this investigation, is placed on the head of a 3-axis handling robot 3 mm above the PCB according the positions described in Fig. 4. The induced voltage measurement is performed is the same way as for the RI measurement.

Fig. 5 shows the voltage measured across the 1 kΩ load placed at the termination of the less coupled line T4. The NFSI is performed at a constant forward power of 10 dBm.

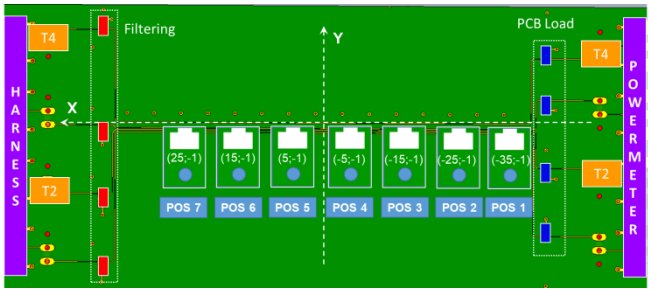

Fig. 4. Immunity probe's positions during NFSI

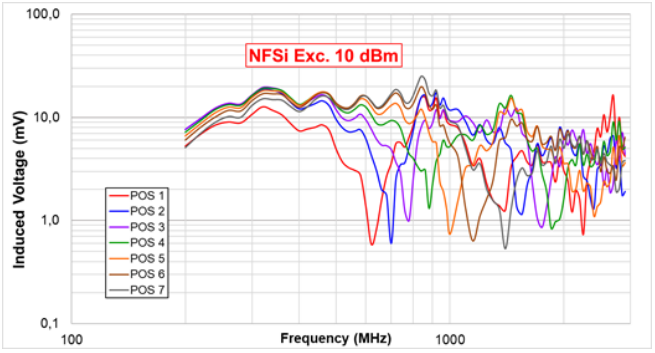

Fig. 5. Induced voltages measured during NFSI on T4 load (Conf #1)

We clearly observe induced voltage minima at frequencies F calculated by (1) where c is the speed of light, ε_{eff} is the effective dielectric constant of the propagation medium, n is a positive integer, and s is the distance between the probe and an open circuit seen on the transmission line at the opposite side of the PCB load:

$$F = (2n+1) * c/(2 * \sqrt{\varepsilon_{eff}} * s) \qquad (1)$$

As the measurement is dependent to the position of the probe, it is mandatory to consider the maximum or the mean value of the induced voltage on all probe's positions.

Fig. 8 shows the maximum value of induced voltages during the NFSI performed at 10 dBm forward power on the loads placed on line T2 and T4 for the Conf#2.

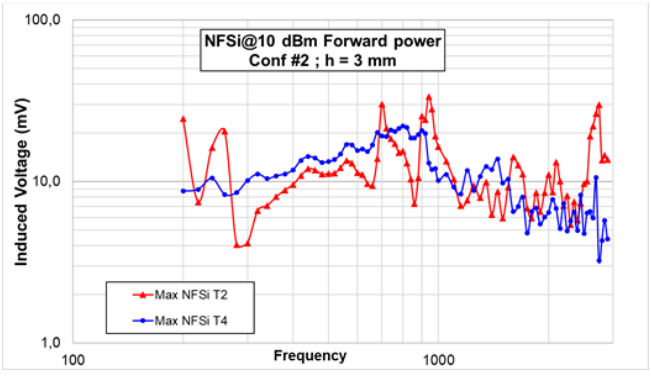

Fig. 6. Induced voltages during the NFSI@10 dBm (Conf#2)

In Fig. 8, the effects of the input capacitance in lower frequencies are not clearly observable. This point could be explained by the relationship stated in [9] between the induced voltage $V(Z_L)$ and the impedance of terminal loads Z_0 and Z_L attached to a electrically-short transmission line described in Fig.7. E-field is not considered because the immunity probe is mainly magnetic up to 1 GHz.

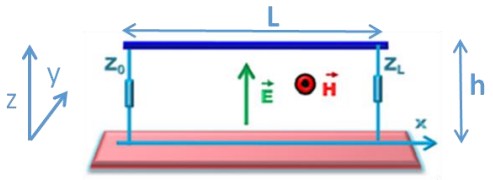

Fig. 7. Irradiation of a transmission line

$$V(Z_L) = \left(\frac{Z_L}{Z_L+Z_0}\right) * j * 2 * \pi * F * \mu_0 * H_y * h * L \qquad (2)$$

In Conf#2, Z_L equals 10 kΩ and Z_0 is constituted by the 10 nF capacitance in parallel with the harness wire termination load (100 Ω) brought back to the PCB input. In lower frequencies, Z_0 is negligible compared to Z_L.

In comparison, Fig. 8 shows the maximum value of induced voltages during the NFSI performed at 10 dBm forward power on the loads placed on line T2 and T4 for the Conf#3. The effect of the capacitance placed in parallel of the load is now observable on the measurement with a 20 dB reduction of the induced voltage in the lower frequencies. These measurements show that NFSI, performed with a magnetic immunity probe, seems to incorrectly consider the components placed upstream the injection probe i.e placed between the input of the trace and the injection probe.

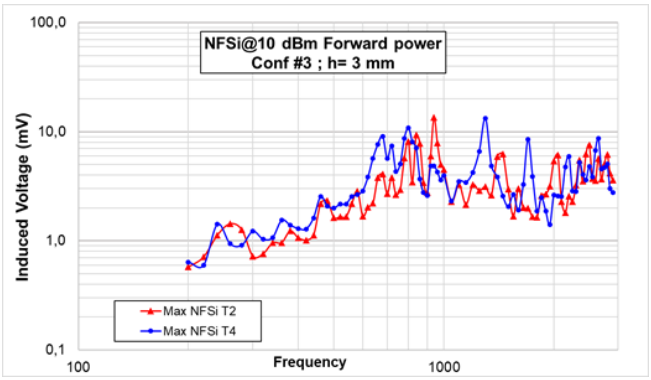

Fig. 8. Induced voltages during the NFSI@10 dBm (Conf#3)

D. RI vs NFSI Raw Measurements Comparison

We propose to compare the NFSI to the RI measurements using a common failure criterion which is a voltage beyond which the equipment is failing. This value will be also used to calibrate the NFSI forward power. In our example, the failure criterion is set to 7 mV for the Conf #1 and to 1 mV for the Conf #2 & 3. The failure criterion allows determining an immunity level equals to the ratio of the induced voltage to the failure criterion. When the induced voltage is below the failure criterion, the value of the immunity level = 1 meaning the test is PASS. Fig. 9 illustrates the comparison of the immunity level for loads placed on lines T2 & T4 between RI@1 V/m and NFSI performed at calibrated power Pcal (7 mV for Conf #1).

We introduce here some merit factors to evaluate the RI immunity level prediction given by the NFSI measurement performed at calibrated power. The first one is the percentage of correct detection of the failure. For each

frequency, the detection is correct when both the RI and NFSI measurements lead to an immunity level =1 (PASS) or to an immunity level < 1 (FAIL). The second one is the percentage of no detection. For each frequency, there is no detection when the RI measurement leads to an immunity level < 1 and the NFSI measurement leads to an immunity level = 1. Finally, the third merit factor is the percentage of false detection. For each frequency, the detection is false when the RI measurement leads to an immunity level = 1 and the NFSI measurement leads to an immunity level < 1. The comparison is made on 71 frequency points between 200 MHz and 2.5 GHz.

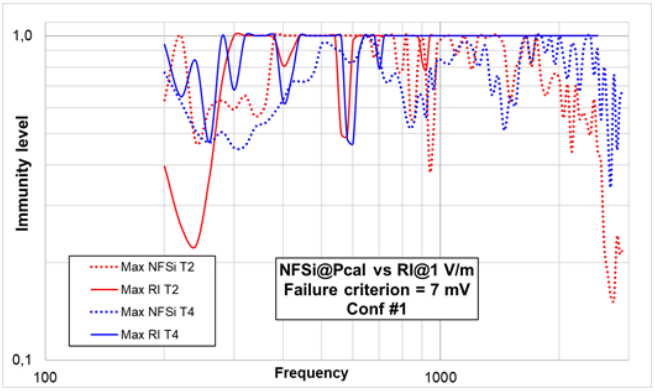

Fig. 9. Comparison of immunity level RI@1 V/m vs NFSI@calibrated power (Conf#1)

Fig. 10 summarizes the merit factors of the prediction built from NFSI measurements performed at calibrated power for loads placed on lines T2, T4 and both configurations. For an industrial need, a satisfying prediction is a correct detection rate > 80 % with a no detection rate < 10 %.

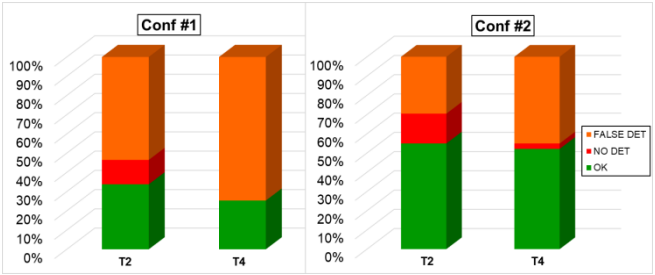

Fig. 10. Merit factors of immunity prediction based on NFSI performed at calibrated power

We observe the correct detection rate is low and close to a random draw. The NFSI measurement performed at forward power calibrated on a 50 Ω microstrip line does not allow a good prediction of the immunity level measured in RI. A method is needed to predict the radiated immunity level in far field from the NFSI measurements in a satisfactory manner.

III. Prediction Methodology

The methodology described in this section has been developed to solve the cases of product redesign which are numerous in automotive industry. Design changes, which require a new qualification of the modified equipment, represent around 40 % of qualification laboratory activities. However, in main cases, design changes are localized and limited to minor PCB layout change, pin to pin compatible component change and/or the addition of filtering passive components. The harness and the load box are not modified. In the rest of this paper, we will call A-version the original equipment version and B-version the modified equipment version. The results of a RI measurement made on A-version are available. The objective of the methodology is to predict the immunity level in RI of the B-version from RI measurements of the A-version and NFSI measurements of A and B-versions.

The methodology is based on the assumption of the linearity of whole system as illustrated in Fig. 11. In (3), the voltage induced on a load Z_c is directly depending on the forward power P_{forw} and on the transmission coefficient S_{21}. Consequently, a change of the layout and/or of impedance placed on the path will be seen in the S_{21} then in the voltage measured in NFSI.

$$V_{ind} = \sqrt{P_{forw}} * \sqrt{Z_c} * |S_{21}| \quad (3)$$

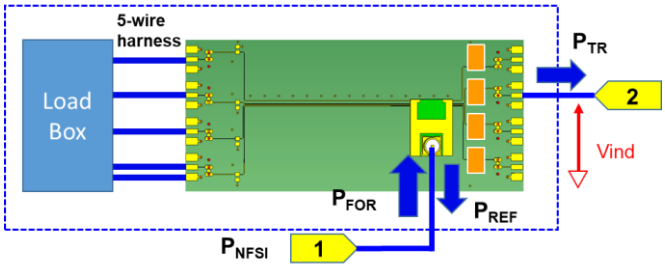

Fig. 11. Representation of whole system by its S-parameters

The different steps of the methodology are described in Fig. 12. Each step will be explained and detailed in the case of layout change.

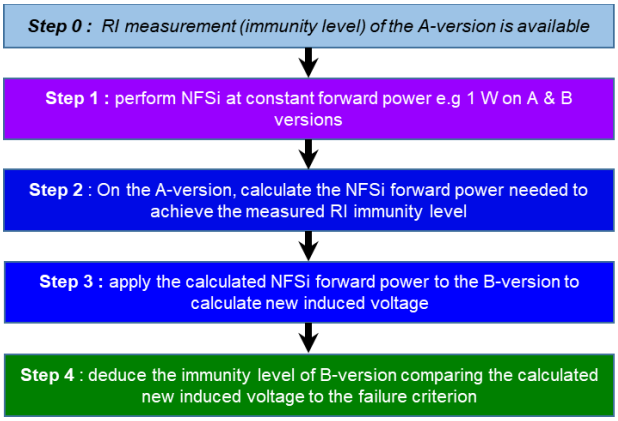

Fig. 12. Prediction methodology steps

A. *Case of Layout Change*

We will study the case of layout change in the Conf #1. The A-version is the case of a function represented by a 1 kΩ placed at the termination of the most coupled line T2. The B-version is the case of the same function placed at the termination of the less coupled line T4. The RI measurement of the A-version leads to an immunity level illustrated by the solid red curve Max RI @1 V/m T2 of the Fig.7a and determined for a failure criterion of 7 mV.

The first step of the method consists in performing a NFSI measurement at constant forward power on both versions.

The only constraint is that the forward power is sufficient for the measured voltage to be within the measuring range of the apparatus. Applying (3), we obtain the following equations where V_{ind} NFSI(A) is the voltage induced during the NFSI measurement on A-version when the forward power P_{NFSI} (A) is applied to the probe and S_{21}(A) is the probe's coupling factor on A-version :

$$|S_{21}(A)| = V_{ind}\ NFSI\ (A)\ /\sqrt{P_{NFSI}(A) * 50} \quad (4)$$

$$|S_{21}(B)| = V_{ind}\ NFSI(B)\ /\sqrt{P_{NFSI}(B) * 50} \quad (5)$$

As the goal of the methodology is to reproduce on the B-version the effects of the E or H-field applied on the A-version during RI measurement, the second step consists in calculating the level of the NFSI forward power to apply to the probe on the A-version $P_{NFSI}\ RI(A)$ to reach the same immunity level as seen during RI measurement. Still applying (1), we obtain (6) where $V_{ind}\ RI(A)$ is the voltage induced on the load during the RI measurement on the A-version when $P_{NFSI}\ RI(A)$ is applied to the probe :

$$|S_{21}(A)| = V_{ind}\ RI\ (A)\ /\sqrt{P_{NFSI}\ RI\ (A) * 50} \quad (6)$$

Using the equality between (4) and (6) we obtain (7):

$$P_{NFSI}\ RI(A) = (\frac{V_{ind}\ RI(A)}{V_{ind}NFSI(A)})^2 * P_{NFSI}(A) \quad (7)$$

Fig. 13 illustrates the NFSI forward power to achieve the same immunity level as during the RI measurement on the A-version.

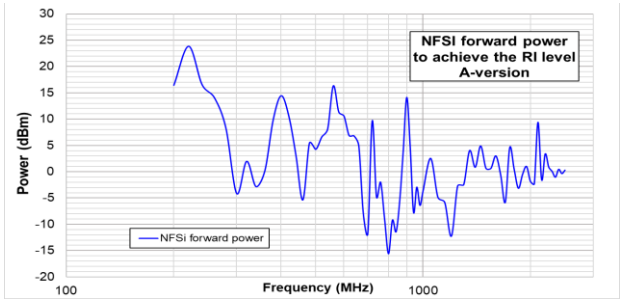

Fig. 13. NFSI forward power to achieve the RI level on A-version

The third step consists in applying to the probe the previously calculated forward power $P_{NFSI}\ RI(A)$ on the B-version. The new induced voltage $NV_{ind}\ NFSI(B)$ is calculated by (8):

$$NV_{ind}NFSI(B) = \sqrt{P_{NFSI}RI(A)} * \sqrt{50} * |S_{21}(B)| \quad (8)$$

Using (5) in (8), we obtain (9):

$$NV_{ind}NFSI(B) = \frac{\sqrt{P_{NFSI}RI(A)}}{\sqrt{P_{NFSI}(B)}} * V_{ind}NFSI\ (B) \quad (9)$$

Fig. 14 shows the comparison of the new induced voltage calculated by the method with the induced voltage measured in RI on B-version for the Conf #1.

Fig. 15 shows the comparison of the immunity level predicted with and without the methodology with the immunity level measured in RI on B-version on the Conf #1. We clearly observe an improvement in the prediction.

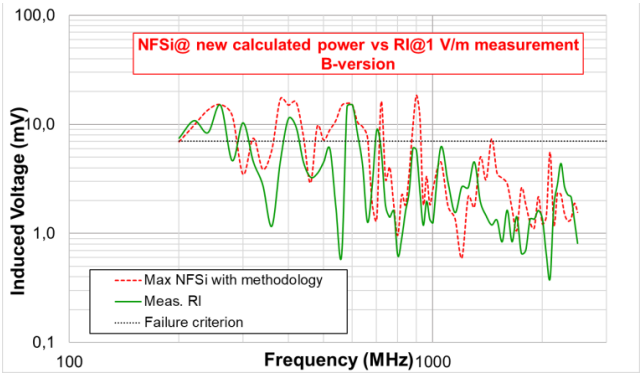

Fig. 14. Comparison of the new induced voltage calculated with the method vs measured induced voltage in RI on B-version (Conf #1)

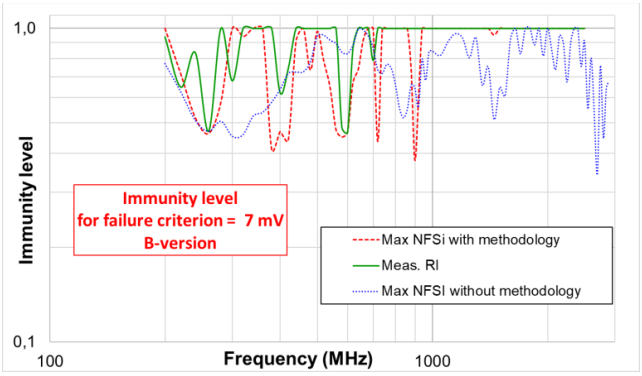

Fig. 15. Comparison of the immunity level predicted with and without the method vs the immunity level measured in RI on B-version (Conf #1)

We also applied the methodology to the same layout change on the Conf #2. Fig. 16 summarizes the merit factors of NFSI prediction for both configurations when the methodology is used or not. Using the methodology, the level of correct detection is > 80%.

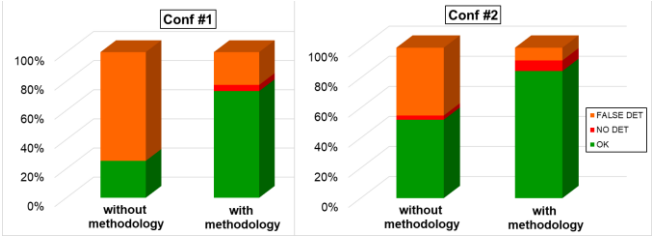

Fig. 16. Comparison of merit factors of the immunity level prediction using the methodology or not in case of layout change

B. Case of Component Change

Now we will study the case of component change. The A-version is the case of a "function" represented by a 1 kΩ placed at the termination of the most coupled line T2 (Conf #1). The B-version is the case of a "function" represented by a 10 kΩ placed at the termination of line T2 and a 10 nF capacitor placed at the input of this same line (Conf #2).

Fig. 17 summarizes the merit factors of NFSI prediction for the change Conf #1 to Conf #2 and for the change Conf #1 to Conf #3 when the methodology is applied or not. The methodology shows no improvement for the change Conf #1 to Conf #2 confirming the fact input capacitance is incorrectly considered by the NFSI measurement. The methodology shows an improvement mainly for the change

Conf #1 to Conf #3 in comparison with the NFSI measurements performed without methodology increasing the correct detection by a factor of 1.22 and decreasing the non-detection by a factor of 2.8.

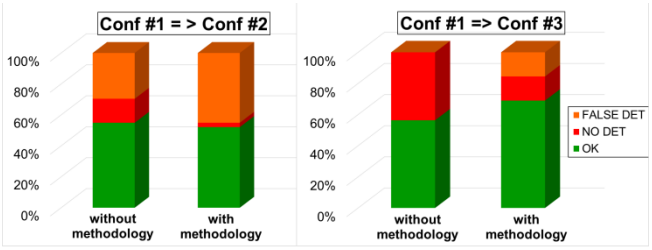

Fig. 17 Comparison of merit factors of the immunity level prediction using the methodology or not in case of component change

Advantage given by the methodology seems low considering the merit factor comparison. Actually, Fig. 18 clearly shows that the rate of correct detection without methodology is close to a random draw while the methodology succeeds in finding the resonances of the harness.

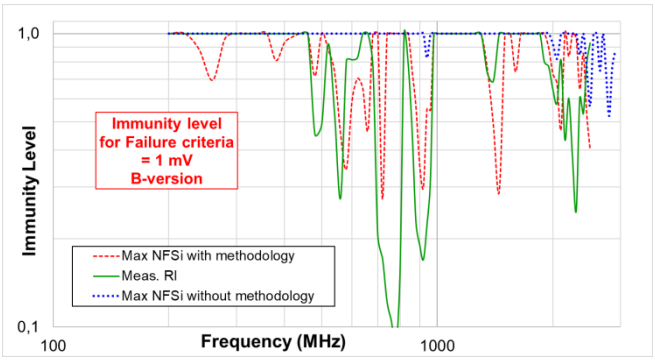

Fig. 18. Comparison of the immunity level predicted with and without the method vs the immunity level measured in RI: Conf #1 to Conf #3

IV. Conclusion and Perspectives

The methodology presented in this paper has been developed to avoid equipment requalification after a design change. The methodology uses NFSI measurements performed at equipped PCB level with wide band probes especially designed to quick investigation. It allows a satisfying prediction of the immunity level in far field of an equipment after a PCB layout or component change from an RI measurement made on the initial version of the equipment and NFSI measurements performed at constant forward power on the initial and final versions of the equipped PCB.

The advantages of the methodology are:

•a correct consideration of the harness resonances seen during the RI measurement,

•as the methodology relies on the linearity of the overall system, the immunity level prediction is fully determined by calculation from initial measurement achieved at constant forward power. This power must be sufficient to stay within the measuring range of the apparatus,

• The immunity level prediction is improved compared to NFSI measurements performed without the methodology. In case of layout change, the correct prediction increases by a factor of 1.6 to 2.9 depending on the case.

The drawbacks of the methodology are mainly linked to those of the NFSI measurement:

•The NFSI measurement, achieved with a magnetic probe, may not correctly consider the components placed upstream of the probe. This is particularly problematic for filtering components placed at connector input. In this case, the NFSI measurement must be performed at the connector level or at the input of the electrical harness. The use of E-Field immunity probe as described in [10] could also be a way to solve the problem.

•The NFSI measurement is sensitive to probe's position especially for the single-ended lines. In the case of long lines, the method considers the maximum value of the measurements performed along the line. The optimization of the number of measurements is a way of improvement. Furthermore, a specific attention must be paid in data processing especially if a component change occurs along the line.

References

[1] Road vehicles - Component test methods for electrical disturbances from narrowband radiated electromagnetic energy - Part 2: Absorber-lined shielded enclosure, ISO 11452-2, 2019

[2] Integrated circuits - Measurement of electromagnetic immunity - Part 9: Measurement of radiated immunity - Surface scan method, IEC TS 62132-9, 2014

[3] D. Castagnet, A. Meresse, G. Duchamp, "ICs electromagnetic susceptibility : comparison between near field injection method and a direct injection method" in *Proc 3rd International Conference on Near Field Imaging and Characterization- ICONIC*, St Louis, USA, 2007, pp 290-295

[4] Integrated circuits - Measurement of electromagnetic immunity 150 kHz to 1 GHz - Part 4: Direct RF power injection method, IEC 62132-4, 2006

[5] Integrated circuits - Measurement of electromagnetic immunity - Part 2: Measurement of radiated immunity - TEM cell and wideband TEM cell method, IEC 62132-2, 2010

[6] O. Kroning, M. Krause, M. Leone, "Near field-Immunity Scan on Printed Circuit Board Level", in *Proc. IEEE 14th Workshop on Signal Propagation on Interconnects - SPI*, Hildesheim, Germany, 2010, pp. 101-102.

[7] A. Boyer, "A Rigorous Method to extrapolate Radiated Susceptibility from Near-Field Scan Immunity" in *Proc. International Symposium on Electromagnetic Compatibility- EMC EUROPE*, Barcelona, Spain, 2019, pp 580-585

[8] A. Boyer, S.Bendhia, A.Durier, "A new Voltage Measurement Probe for investigating Radiated Immunity Test" in Proc. International Symposium on Electromagnetic Compatibility- EMC EUROPE, Roma, Italy, 2020, pp 1-5

[9] C.R. Paul, *Analysis of multiconductor transmission lines*, John Wiley & Sons, 1994, chapter 11

[10] A.Durier, S. Bendhia, T. Dubois, "Study of the Coupling of Wide Band Near Field Scan Probe dedicated to the Investigation of the Radiated Immunity of Printed Circuit Boards", in *Proc. IEEE 23th Workshop on Signal and Power Integrity - SPI*, Chambéry, France, 2019, pp. 1-4.